Neural Sequenced Active Fault Management for Resilient Microgrids

Lizhi Wang, *Member, IEEE*, Priyanka Mishra, *Member, IEEE*, Ella Chou and Peng Zhang, *Senior Member, IEEE*

2024 IEEE Power & Energy Society General Meeting (PESGM) | 979-8-3503-8183-2/24/$31.00 ©2024 IEEE | DOI: 10.1109/PESGM51994.2024.10688993

***Abstract*—Neural sequenced active fault management (NSAFM) is devised to maintain the microgrids' reliable operation and also to properly control microgrids' and renewable energy's sequence current under balanced or unbalanced faults. The main contributions include 1) a neural sequenced control framework for microgrids with fault ride-through capability; 2) an optimization-based sequenced AFM formulated to regulate the sequence current of renewable energy under unbalanced faults; 3) a learning-based sequenced AFM control algorithm, which transfers computation from online optimization to offline training. The deployable neural sequenced AFM scheme is thoroughly verified on a microgrid with a single-phase-to-ground fault using hardware-in-the-loop (HIL) in a Real-Time Digital Simulator (RTDS) environment, and the experimental results show that the proposed method can significantly improve system resilience regarding the fault current contribution.**

***Index Terms*—Microgrid control, fault management, learning-based control, HIL, optimization.**

I. Introduction

THE imperatives of fault ride-through for distributed energy resources (DERs), which mandate that renewable generators maintain grid connection and power output during fault conditions, are paramount in ensuring grid stability [1]. Active Fault Management (AFM) is instrumental in enhancing microgrids' ability to ride through such disturbances. Specifically, AFM can 1) enable microgrids' ride-through capabilities, which is to keep connected to the main grid during faults to prevent instability caused by loss of large generation, 2) regulate the total fault contributions by coordinating heterogeneous microgrids and DERs, which is to protect equipment from overcurrents damage and to minimize updating for the relay, and 3) reduce voltage ripples during fault occurrence and fault clearance [2]. Existing fault managements for microgrids mostly focus on controlling one variable, such as fault currents, while other critical variables, such as power balance and power ripples, are not controlled [3], [4]. Our previous work [5] allow only positive sequence current during an unbalanced fault, which is not a desirable condition for a system with negative sequence overcurrent relays. Therefore, efficacious microgrid fault control that can assure the sequence of current regulation and massive DER coordination is needed.

The problem of AFM can be formulated as a constrained nonlinear optimization problem [5], [6]. Compared with feedback control, which focuses on certain variables while ignoring other variables [7], [8], [9], optimization can consider multiple variables, putting them as objectives and constraints. Our previous work [10] pioneered the investigation into AFM using centralized optimization for a single microgrid, and a distributed and asynchronous surrogate Lagrangian relaxation (DA-SLR) algorithm for networked microgrids(NMs).

Negative sequence components pose a significant threat to electrical machinery, potentially causing overheating in generators and motors which can lead to equipment degradation, reduced operational efficiency, and elevated safety hazards. To mitigate these issues, microgrids are equipped with negative sequence current protection systems designed to rapidly detect and rectify such imbalances. Nonetheless, two predominant challenges persist in current methodologies [11]: (I) the absence of an AFM approach capable of generating both positive and negative sequence currents in the event of an unbalanced fault, and (II) a deficiency in effective strategies that guarantee real-time performance in microgrid fault management.

To bridge the gap, this paper establishes a neural-sequenced active fault management (NSAFM) for resilient microgrids. We first construct a neural sequenced current control framework for microgrid, and then we construct sequenced AFM as an optimization-based current control problem to generate positive as well as negative sequence currents during an unbalanced fault. Finally, a machine learning method [12] is leveraged to replace the optimization-based AFM and achieve the control goal in milliseconds. The trained neural networks are verified in controller HIL real-time simulation.

The remainder of this paper is organized as follows. Section II presents the sequenced active fault management with sequenced current control. Section III formulates optimization-based sequenced active fault management problem. Section IV introduces the implementation of NSAFM. Section V presents case studies. Section VI provides the conclusion of the paper.

II. Sequenced active fault management

A. Motivation of sequenced AFM

AFM aims at decreasing microgrid's contributions in the main grid's fault currents (Fig. 1(a)). Fault current contributions mean how large fault currents' amplitudes, $|I_f^T|$, have been increased because of the integration of microgrid. Because total fault currents are vector additions of the main

This work was supported in part by the National Science Foundation under Grant No. OIA-2134840. This work relates to Department of Navy award N00014-22-1-2001 issued by the Office of Naval Research. The United States Government has a royalty-free license throughout the world in all copyrightable material contained herein.

L. Wang and E. Chou are with Siemens Technology, Princeton, NJ, USA (e-mail: wang.lizhi@siemens.com).

P. Mishra, W. Wan and P. Zhang are with the Department of Electrical and Computer Engineering, Stony Brook University, NY, USA.

grid's fault currents and microgrid' fault currents as shown in Fig. 1(b). Total fault currents and the main grid's fault currents can have the same amplitude even when microgrid' fault currents are not zero, which suggests that the integration of micorgrid has a minimal impact on the main grid. Achieving this balance involves precise adjustments to the amplitude and phase angles of the currents of microgrids. However, it is important to note that microgrids commonly incorporate negative overcurrent relays, necessitating careful control over both the positive and negative components of the current in AFM.

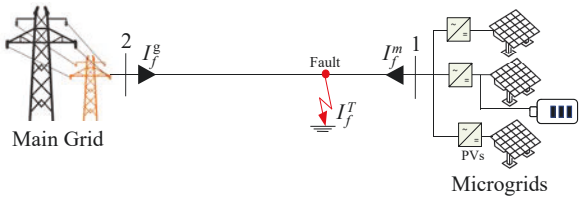

(a) Protection for microgrids integrated system

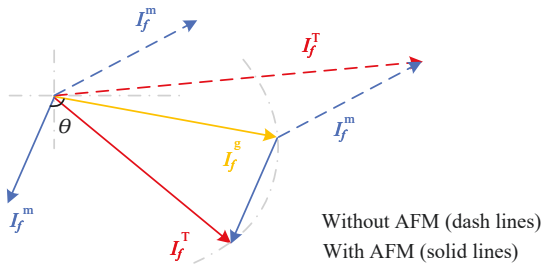

(b) Relationship of fault currents without and with AFM

Fig. 1: Motivation of active fault management

B. Sequence current control scheme

The sequenced current control scheme, designed to regulate the sequence current upon receiving a control signal from the AFM, is introduced.

With the three-phase unbalanced input voltage (E_i^{abc}) and fault currents (I_i^{abc}) without zero sequences, the apparent power can be expressed as the orthogonal sum of positive and negative sequences, such that

$$S_i = (e^{j\theta}E_{dq}^{+} + e^{-j\theta}E_{dq}^{-})(e^{j\theta}I_{dq}^{+} + e^{-j\theta}I_{dq}^{-}) \tag{1}$$

where $+$ and $-$ denote the positive and negative components separately. Separating the real power and the reactive power of the three phases, we obtain, [13]:

$$\begin{cases} P(t) = P_0 + P_{c2}cos(2\theta) + P_{s2}sin(2\theta) \\ Q(t) = Q_0 + Q_{c2}cos(2\theta) + Q_{s2}sin(2\theta) \end{cases} \tag{2}$$

where

$$\begin{cases} P_0 = 1.5(E_d^+I_d^+ + E_q^+I_q^+ + E_d^-I_d^- + E_q^-I_q^-) \\ P_{c2} = 1.5(E_d^+I_d^- + E_q^+I_q^- + E_d^-I_d^+ + E_q^-I_q^+) \\ P_{s2} = 1.5(E_d^-I_d^+ - E_q^-I_q^+ - E_q^+I_d^- + E_d^+I_q^-) \\ Q_0 = 1.5(E_q^+I_d^+ - E_d^+I_q^+ + E_q^-I_d^- - E_d^-I_q^-) \\ Q_{c2} = 1.5(E_q^+I_d^- - E_d^+I_q^- + E_q^-I_d^+ - E_d^-I_q^+) \\ Q_{s2} = 1.5(E_d^+I_d^- + E_q^+I_q^- - E_d^-I_d^+ - E_q^-I_q^+) \end{cases}$$

Here, superscripts $+$ and $-$ refer to positive and negative sequences. Subscripts d and q refer to direct and quadrature axis components. The double-line frequency power coefficients P_{c2}, P_{s2} Q_{c2}, and Q_{s2} are caused by the voltage unbalance, which causes fluctuations in the DC-link voltage, i.e. second-order harmonic ripple will appear. Therefore, to keep a constant DC-link voltage, the power coefficients P_{c2} and P_{s2} have to be nullified.

Expressing the power coefficients in the matrix form, we obtain

$$\frac{2}{3}\begin{bmatrix} P_0 \\ Q_0 \\ P_{s2} \\ P_{c2} \end{bmatrix} = \begin{bmatrix} E_d^+ & E_q^+ & E_d^- & E_q^- \\ E_q^+ & -E_d^+ & E_q^- & -E_q^- \\ E_q^- & -E_d^- & -E_q^+ & E_d^+ \\ E_d^- & E_q^- & E_d^+ & E_q^+ \end{bmatrix} \begin{bmatrix} I_d^+ \\ I_q^+ \\ I_d^- \\ I_q^- \end{bmatrix} \tag{3}$$

Removing dc-link voltage ripple, necessitates making $\frac{2}{3}[P_0Q_0P_{s2}P_{c2}] = [\frac{2}{3}P_0Q_000]^T$. Therefore, the control objectives I^* can be satisfied by choosing currents such that

$$\begin{bmatrix} I_d^+ \\ I_q^+ \\ I_d^- \\ I_q^- \end{bmatrix}^* = \frac{2}{3}\begin{bmatrix} E_d^+ & E_q^+ & E_d^- & E_q^- \\ E_q^+ & -E_d^+ & E_q^- & -E_q^- \\ E_q^- & -E_d^- & -E_q^+ & E_d^+ \\ E_d^- & E_q^- & E_d^+ & E_q^+ \end{bmatrix} \begin{bmatrix} P_0 \\ Q_0 \\ 0 \\ 0 \end{bmatrix} \tag{4}$$

For unbalanced input voltage, the control objectives are achieved by flowing negative-sequence currents. In the context of this control scheme, the current reference is derived using a PQ control strategy during standard operation. In the subsequent section, we will delve into the methodology for formulating current references via a sequenced AFM approach when addressing fault conditions.

C. Resilience metric for sequenced AFM

AFM is devised to improve microgrid resilience against large disturbances,e.g. balanced and unbalanced faults. A resilience metric [14] is utilized to quantify the system resilience:

$$\xi = 0.5(\xi_1 + \xi_2) \tag{5}$$

$$\xi_1 = \frac{d_1}{d_0} \tag{6}$$

$$\xi_2 = \frac{\int_{t_1}^{t_2} d_t dt}{d_0(t_2 - t_1)} \tag{7}$$

where ξ is the resilience. ξ_1 is the invulnerability and ξ_2 is the recovery. d_1 is the value of the variable of interest during disturbance and d_0 is the variable's values before disturbance. t_1 and t_2 are the disturbance happening time and clearing time, respectively. ξ, ξ_1 and ξ_2 are all in the range of 0 to 1. Larger ξ means the system is more resilient.

III. Optimization-based Sequenced Active Fault Management

AFM is formulated as a nonlinear constrained optimization problem given in equations (8):

$$\min \ \alpha_1F_1 + \alpha_2F_2 + \alpha_3F_3 + \alpha_4F_4, \quad \boldsymbol{\alpha} \in [0,1] \tag{8}$$

where $\boldsymbol{\alpha} = \{\alpha_1, \alpha_2, \alpha_3, \alpha_4\}$ are weighting factors between different parts in the objective function.

The objective function has four parts:

1) F_1 are fault current contributions, the magnitude difference between fault currents from the main grid and total fault currents.

$$F_1 \equiv \left| \frac{[\mathrm{Re}(\mathbf{I}^M_{dq0}+\mathbf{I}^m_{dq})]^2+[\mathrm{Im}(\mathbf{I}^M_{dq0}+\mathbf{I}^m_{dq})]^2}{[\mathrm{Re}(\mathbf{I}^M_{dq0})]^2+[\mathrm{Im}(\mathbf{I}^M_{dq0})]^2} - 1 \right| \quad (9)$$

Superscripts M, m indicate variables related to the main grid and all microgrids, respectively. $\mathbf{I}^M_{dq0}, \mathbf{I}^m_{dq}$ are fault currents from the main grid and from the microgrid, respectively. $\mathbf{I}^M_{dq0} + \mathbf{I}^m_{dq}$ are total fault currents.

2) F_2 is microgrid negative sequence current magnitude.

$$F_2 \equiv -\sum_{i=1}^{N} ([\mathrm{Re}(\mathbf{I}^{i-}_{dq})]^2 + [\mathrm{Im}(\mathbf{I}^{i-}_{dq})]^2) \quad (10)$$

Subscript i indicates variables related to DER $i \in \{1, 2, ..., N\}$. AFM aims to increase negative sequence current, which is desired for microgrids with negative sequence current relays.

3) F_3 is microgrid reactive power output:

$$F_3 \equiv -\sum_{i=1}^{N} Q_i \quad (11)$$

4) F_4 is power ripples:

$$F_4 \equiv \sum_{i=1}^{N} \frac{R_i}{P_i^2} \quad (12)$$

Power ripples are to be minimized.

where $P_i \equiv 1.5(E^{i+}_d I^{i+}_d + E^{i+}_q I^{i+}_q + E^{i-}_d I^{i-}_d + E^{i-}_q I^{i-}_q)$, $Q_i \equiv 1.5(E^{i+}_q I^{i+}_d - E^{i+}_d I^{i+}_q + E^{i-}_q I^{i-}_d - E^{i-}_d I^{i-}_q)$ and $R_i \equiv 2.25[(P_i)^2 + (Q_i)^2]$. P_i and Q_i are active and reactive power outputs from microgrid i.

AFM has two types of constraints: system-wide coupling constraints and local constraints. System-wide coupling constraints contain decision variables of more than one DER, and local constraints only involve decision variables of one DER.

1) Coupling constraints: tie line safety rating constraint. This means the microgrid's output currents should be less than a safety threshold, I^m_{Rated}:

$$[\mathrm{Re}(\mathbf{I}^m_{dq})]^2 + [\mathrm{Im}(\mathbf{I}^m_{dq})]^2 \leq (I^m_{Rated})^2. \quad (13)$$

2) Local constraint 1: DER-wise safety rating constraint. Each DER's output currents during fault should be less than its own safety rating, I^i_{Rated}:

$$[\mathrm{Re}(\mathbf{I}^i_{dq})]^2 + [\mathrm{Im}(\mathbf{I}_{dq})^i]^2 \leq (I^i_{Rated})^2. \quad (14)$$

3) Local constraint 2: zero sequence components elimination constraint. This constraint means the sum of each DER's three-phase currents is zero. This constraint is required if a microgrid's interface converter or nearby transformer does not allow zero-sequence currents:

$$\textstyle\sum_{f\rho} \mathbf{I}^i_{f\rho} = \mathbf{0}. \quad \forall \rho \in \{a, b, c\} \quad (15)$$

$f\rho$ denotes the faulty phase ρ.

4) Local constraint 3: battery power buffer constraint. For DER to have a battery as a buffer, the power output difference between before faults and after faults should be smaller than the power rating of the battery. Otherwise, it is beyond the battery's capability to keep a power balance:

$$(P_i - P^{bf}_i)^2 \geq (P^{bty}_i)^2. \quad (16)$$

P^{bf}_i denotes the power output before fault and P^{bty}_i is the power rating of the battery.

5) Local constraint 4: Reactive power constraint. We derive that the reactive power of the microgrid should be larger than zero to supply the leading current during unbalanced fault:

$$Q_i \geq 0. \quad (17)$$

IV. Neural Sequenced AFM

Optimization-based AFM would lead to extensive computation time if a larger scale system with complex objectives and constraints is considered. The optimization-based fault management algorithm needs more than 100 ms to output reference values, and the fault management is expected to have compromised performance or even fail. In this section, we use a general regression neural network (GRNN) to replace the optimization-based AFM. First, the training data are achieved by the optimization. Regression means estimating relationships between outputs and inputs. In the case of AFM, inputs are system status, such as microgrid voltages, fault voltages, fault currents, power, etc. Outputs are reference values for the DER's output currents. Previously, outputs were decided by optimizations used in AFM. Here, neural works are used to approximate the optimization function. The used neural network is feed-forward with a multi-layer perceptron without feedback between layers as shown in Fig. 2.

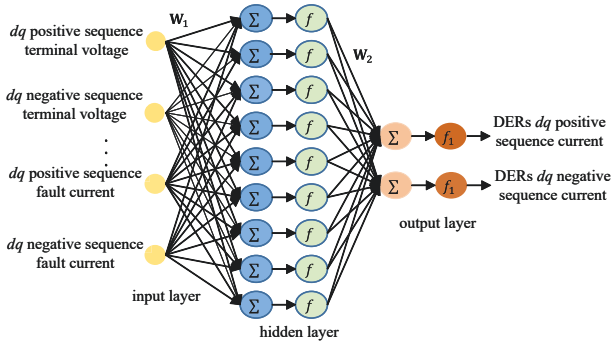

Fig. 2: GRNN Learning scheme.

Fig. 3 presents the architecture of the NSAFM which can regulate positive sequence and negative sequence currents reference separately. In this control architecture, the inverter works as a regular grid following the controller, which generates as much power as is regulated without faults. When faults happen, the AFM will switch in, and sequence current references will be generated to regulate the positive and negative sequence current and satisfy the objective of AFM. The inverter will follow the current reference i^*_n in the normal operation condition. The learning-based control signals of all the N DERs, i.e., $\boldsymbol{u} = [i^{+*}_d, i^{+*}_q, i^{+*}_d, i^{-*}_q]^T$, are functionally formulated as a neural network $\boldsymbol{u} = \boldsymbol{\pi}_\varphi(\boldsymbol{x})$, where $\boldsymbol{\pi}$ denotes the neural network describing the control policy; $\boldsymbol{u}$, $\boldsymbol{x}$ and φ respectively denote the output, input, and weights of the neural network.

V. Case Study

The neural sequence active fault management is tested using a typical microgrid (Fig.4) in a controller hardware-in-the-loop

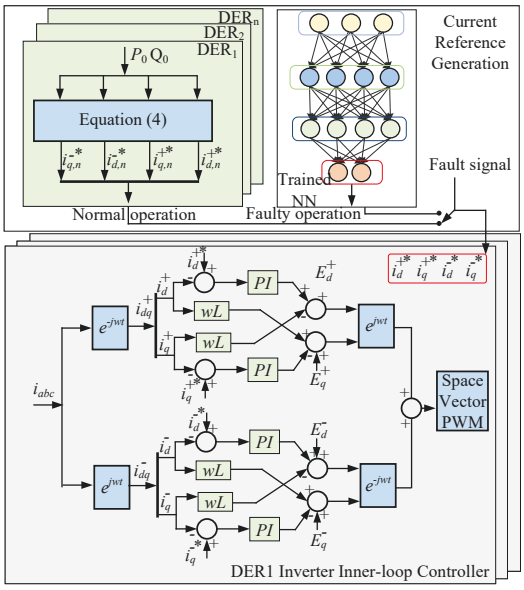

Fig. 3: Structure of the neural hierarchical control of microgrids.

(HIL) test environment [15]. DER 1 and microgrid 3 have DC-link batteries; DER 2 does not have batteries; Those DERs connect to the main grid by power converters.

For the setup of controller hardware-in-the-loop (HIL) real-time simulation, the learning-based controller algorithms run on a personal computer or server, and power grids are run in RTDS simulators.

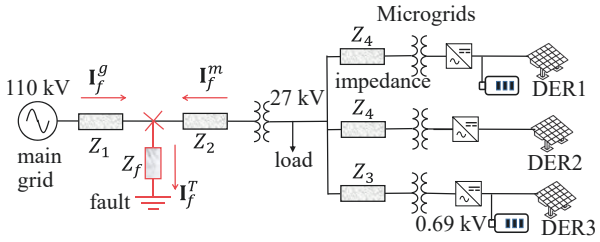

Fig. 4: Diagram of studied system.

A. Single-phase-to-ground faults

This subsection validates the efficacy of the NSAFM method under a typical single-phase-to-ground fault. A single-phase-to-ground fault happens at phase a on the 110 kV grid, as shown in Fig. 4. The fault happens at 0.1s. To investigate system performance under an unbalanced fault, the fault is simulated until 0.5s.

1) Without AFM: The system performance without AFM is shown in this subsection. DERs in microgrids are in power control mode during faults, outputting the same active power and reactive power while maintaining currents within safety ratings. Fig. 5 shows results without AFM, including currents at fault locations, and current contributions. The total to-ground fault currents $\mathbf{I}_a^M+\mathbf{I}_a^m$ and fault currents from the main grid $\mathbf{I}_a^M$ have magnitudes of 200.2 A and 162.4 A, respectively. Microgrids' current contributions are 37.8 A or 18.9%.

2) With NSAFM: The trained neural networks, act as fault management algorithms for microgrid runs on a personal

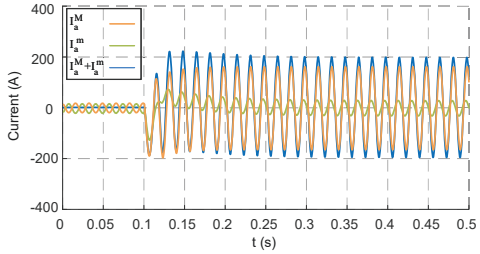

(a) phase a currents at the fault location. $\mathbf{I}_a^M+\mathbf{I}_a^m$, $\mathbf{I}_a^M$ and $\mathbf{I}_a^m$ are total fault currents to the ground, fault currents from the main grid and fault currents from microgrids, respectively.

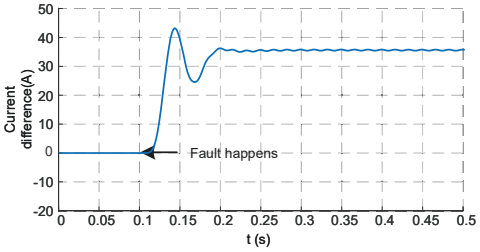

(b) The magnitude difference between $\mathbf{I}_a^M+\mathbf{I}_a^m$ and $\mathbf{I}_a^M$, i.e., $\left|\mathbf{I}_a^M+\mathbf{I}_a^m\right|-\left|\mathbf{I}_a^M\right|$, which are also fault current contributions from microgrids.

Fig. 5: Results for single-phase-to-ground faults without AFM.

laptop. Our previous work shows that the two-way communication time between the simulator and controller is about 1.8 ms [11], which is reasonable for fault management. Fig. 6 shows fault currents at fault locations, and the magnitude difference between total fault currents and fault currents from the main grid, i.e., $\left|\left|\mathbf{I}_a^M+\mathbf{I}_a^m\right|-\left|\mathbf{I}_a^M\right|\right|$. The total fault currents and fault currents from the main grid are 183.6 A and 176.1 A, respectively and thus microgrids' current contributions are 7.5 A or 4.1%. The magnitude difference is minimized as close to 0 as possible.

B. Sequence current analysis

Figure 7 illustrates the negative sequence currents in a microgrid with and without the implementation of NSAFM. Notably, the magnitude of the negative sequence current from the microgrid with NSAFM is double that of the microgrid lacking NSAFM. This observation underscores the capability of NSAFM to generate a higher negative sequence current, which can enhance the performance of microgrids equipped with negative sequence current relays.

Table I lists comparisons of system performance with and without NSAFM. Metrics for comparison include response time, fault current contributions, DER reactive power output, and negative sequence current. It can be seen that NSAFM can achieve nearly real-time performance and generate more reactive power and negative sequence current, which is crucial for the accurate detection and compensation under unbalanced conditions. Critically, the NSAFM-equipped systems manage to suppress fault current contributions to lower levels, which mitigates the risk of damage to electrical components and improves system resilience.

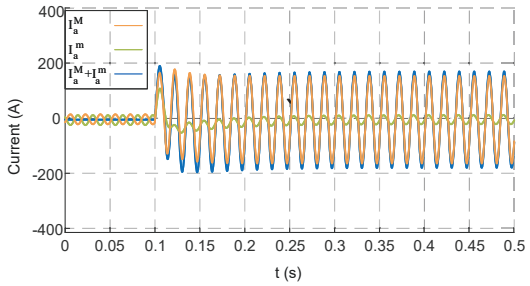

(a) phase a currents at the fault location. $\mathbf{I}_a^M + \mathbf{I}_a^m$, $\mathbf{I}_a^M$ and $\mathbf{I}_a^m$ are total fault currents to the ground, fault currents from the main grid and fault currents from microgrid, respectively.

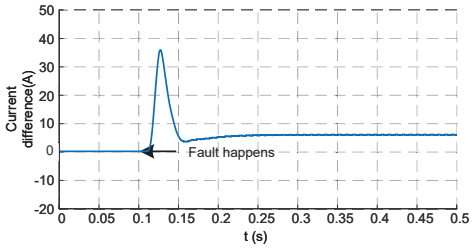

(b) The magnitude difference between $\mathbf{I}_a^M + \mathbf{I}_a^m$ and $\mathbf{I}_a^M$, i.e., $\left|\mathbf{I}_a^M + \mathbf{I}_a^m\right| - \left|\mathbf{I}_a^M\right|$, which are also fault current contributions from microgrid.

Fig. 6: Results for single-phase-to-ground faults with learning-based AFM.

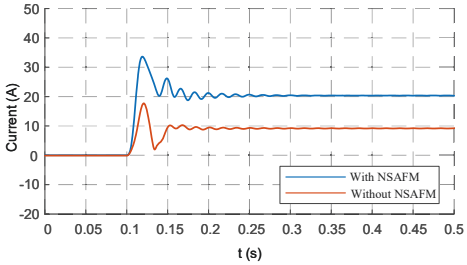

Fig. 7: Negative sequence current with and without NSAFM.

Table II shows resilience metrics for current contributions ($t_1 = 0.1$, $t_2 = 0.5$), and the values are calculated based on Fig.6(b) and Fig.5(b). The results show that the NSAFM can significantly improve system resilience regarding the fault current contribution.

VI. Conclusion

This paper presents a neural sequenced active fault management to achieve real-time safety assurance for microgrids and the main grid during unbalanced faults. The approach works reliably for grid fault currents comparable to microgrid fault current contribution irrespective of the topology of the system. Different from existing phase quantities based active fault management method, microgrids with the proposed sequenced approach provide positive as well as negative sequence currents during unbalanced faults. The generated negative sequence currents can be used for Siemens protection relays on microgrid side. Future work will exploit the devised method in networked microgrids under more complicated system operations.

TABLE I: System performance comparison with/without NSAFM

Metrics	NSAFM	Without AFM
Fault current contributions	4.7%	16.7%
Response time (ms)	5	≤ 3.0
DER1 reactive power (MVAR)	0.2	0
$\lvert I^{m-}\rvert$(A)	21.2	8.5

TABLE II: Resilience metrics for current contributions

Metric	With NSAFM	Without AFM
Invulnerability	82.5%	46.0%
Recovery	80.0%	43.0%
Resilience	81.25%	44.5%

References

[1] D. G. Photovoltaics and E. Storage, "Ieee standard for interconnection and interoperability of distributed energy resources with associated electric power systems interfaces," *IEEE Std*, vol. 1547, pp. 1547–2018, 2018.

[2] L. Wang, S. Zhang, Y. Zhou, C. Fan, P. Zhang, and Y. A. Shamash, "Learning-based, safety and stability-certified microgrid control," in *2023 IEEE Power & Energy Society General Meeting (PESGM)*, pp. 1–5, 2023.

[3] S. Gupta, S. Mukhopadhyay, A. Banerji, and S. K. Biswas, "Fault management in isolated microgrid," in *2018 IEEE International Conference on Power Electronics, Drives and Energy Systems (PEDES)*, pp. 1–6, 2018.

[4] P. V. Dahiwale and N. M. Pindoriya, "Review on fault management in hybrid microgrid," in *2019 IEEE Region 10 Symposium (TENSYMP)*, pp. 415–422, 2019.

[5] P. Zhang, *Networked microgrids*. Cambridge University Press, 2021.

[6] W. Wan, Y. Li, B. Yan, M. Bragin, J. Philhower, P. Zhang, P. Luh, and G. Warner, "Active fault management for microgrids," in *IECON 2018 - 44th Annual Conference of the IEEE Industrial Electronics Society*, pp. 3815–3820, 2018.

[7] L. Ortiz, J. W. González, L. B. Gutierrez, and O. Llanes-Santiago, "A review on control and fault-tolerant control systems of ac/dc microgrids," *Heliyon*, vol. 6, no. 8, p. e04799, 2020.

[8] E. Buraimoh, I. E. Davidson, and F. Martinez-Rodrigo, "Fault ride-through enhancement of grid supporting inverter-based microgrid using delayed signal cancellation algorithm secondary control," *Energies*, vol. 12, no. 20, p. 3994, 2019.

[9] J. C. Rosas-Caro, P. M. García-Vite, A. Rodríguez, A. Mendoza, A. Alejo-Reyes, E. Cuevas, and F. Beltran-Carbajal, "Differential evolution based algorithm for optimal current ripple cancelation in an unequal interleaved power converter," *Mathematics*, vol. 9, no. 21, p. 2755, 2021.

[10] W. Wan, M. A. Bragin, B. Yan, Y. Qin, J. Philhower, P. Zhang, and P. B. Luh, "Distributed and asynchronous active fault management for networked microgrids," *IEEE Transactions on Power Systems*, vol. 35, no. 5, pp. 3857–3868, 2020.

[11] W. Wan, P. Zhang, M. A. Bragin, and P. B. Luh, "Safety-assured, real-time neural active fault management for resilient microgrids integration," *iEnergy*, vol. 1, no. 4, pp. 453–462, 2022.

[12] L. Wang, S. Zhang, Y. Zhou, C. Fan, P. Zhang, and Y. A. Shamash, "Physics-informed, safety and stability certified neural control for uncertain networked microgrids," *IEEE Transactions on Smart Grid*, pp. 1–1, 2023.

[13] H.-S. Song and K. Nam, "Dual current control scheme for pwm converter under unbalanced input voltage conditions," *IEEE Transactions on Industrial Electronics*, vol. 46, no. 5, pp. 953–959, 1999.

[14] R. E. Giachetti, D. L. Van Bossuyt, W. W. Anderson, and G. Oriti, "Resilience and cost trade space for microgrids on islands," *IEEE Systems Journal*, vol. 16, no. 3, pp. 3939–3949, 2021.

[15] L. Wang, Y. Qin, Z. Tang, and P. Zhang, "Software-defined microgrid control: The genesis of decoupled cyber-physical microgrids," *IEEE Open Access Journal of Power and Energy*, vol. 7, pp. 173–182, 2020.